SAND98-2398C

POST TEST ANALYSIS OF A PCCV MODEL DYNAMICALLY TESTED UNDER SIMULATED DESIGN-BASIS EARTHQUAKES

Randy J. James, Liping Zhang and Yusef R. Rashid[1]
Jeff Cherry[2], Nilesh Chokshi[3], and Shiziso Tsurumaki[4]

ABSTRACT

In a collaborative program between the United States Nuclear Regulatory Commission (USNRC) and the Nuclear Power Engineering Corporation (NUPEC) of Japan under sponsorship of the Ministry of International Trade and Industry, the seismic behavior of Prestressed Concrete Containment Vessels (PCCV) is being investigated. A 1:10 scale PCCV model has been constructed by NUPEC and subjected to seismic simulation tests using the high performance shaking table at the Tadotsu Engineering Laboratory. A primary objective of the testing program is to demonstrate the capability of the PCCV to withstand design basis earthquakes with a significant safety margin against major damage or failure. As part of the collaborative program, Sandia National Laboratories (SNL) is conducting research in state-of-the-art analytical methods for predicting the seismic behavior of PCCV structures, with the eventual goal of understanding, validating, and improving calculations related to containment structure performance under design and severe seismic events. With the increased emphasis on risk-informed regulatory focus, more accurate characterization (less uncertainty) of containment structural and functional integrity is desirable. This paper presents results of post-test calculations conducted at ANATECH to simulate the design level scale model tests.

INTRODUCTION

The current practice in the U.S. is to employ linear analyses when establishing the behavior of a containment structure to design level seismic hazards. Typically, modal superposition or time integration procedures are used with lumped mass and beam element models to determine peak displacements and stress levels. For situations where tensile cracking in concrete is likely, cracked-section properties are used to account for reduced stiffness due to cracking. However, the structural frequency shift due to exaggerated stiffness reduction inherent in the cracked-section assumption may cause significant changes in the overall response of the analytical model for a given frequency content of the seismic event. Because the structural

[1]ANATECH Corp., San Diego, CA, USA
[2]Sandia National Laboratory, Albuquerque, NM, USA
[3]US Nuclear Regulatory Commission, Washington, DC, USA
[4]Nuclear Power Engineering Corporation, Tokyo, Japan

DISCLAIMER

response depends on the progressive nature of cracking, the results of such linear models and cracked-section assumptions can be either overly conservative or nonconservative, depending on the intensity of the earthquake motion.

The current U.S. design philosophy aims at linear response while accepting that some nonlinear behavior is inevitable for concrete sections subjected to design level earthquakes. As the target levels for predicted ground motion potentials increase, the need for quantification and verification of the safety margins for these structures becomes clear. With the ever increasing power of affordable computer systems and the advances in concrete constitutive modeling software, it is possible to replace simple methods with detailed continuum modeling of concrete containment structures. The large scale model tests conducted by NUPEC provide valuable data for benchmarking and evaluating such analytical models.

The PCCV scale model shown in Figure 1 was developed by NUPEC as a balance between the limitations of the shake table capacity and the level of construction detailing that adequately represents the structural behavior. The overall geometry is scaled at 1:10 while the concrete wall thickness is 1:8 and the steel liner and anchorages are 1:4. The dome portion of the PCCV is replaced with a thick, flat concrete cap, and added weights are attached to match the fundamental frequency of the model as well as the shear stress at the wall-basemat juncture to that of the prototype. The target input accelerations for the tests are based on response spectra for realistic earthquake records, adjusted in frequency and amplitude consistently with scaling laws to simulate a "scaled" earthquake. The model is first subjected to a series of low level input to develop transfer functions and fundamental frequencies, and then a series of design level seismic tests are conducted. The S1 and S2 level earthquake inputs referred to herein roughly correspond to the Operating Basis Earthquake (OBE) and Safe Shutdown Earthquake (SSE) used in U.S. design. For these tests, the target S1 level input has a peak horizontal magnitude of .28g and a peak vertical amplitude of .13g. The target S2 level input has peak amplitudes of .43g and .21g for the horizontal and vertical components, respectively. For each seismic level, the model is tested for each component individually followed by the combined horizontal and vertical components. After the S2(H+V) test (S2 level seismic input with combined horizontal and vertical components), the model is also subjected to the design condition of S1(H+V) combined with internal pressure simulating a loss of coolant accident (LOCA). The internal pressure for the LOCA condition used in the analysis is 56.9 psi ($4kg/cm^2$). In this paper, post-test simulations of the S1(H+V), S2(H+V), and S1(H+V) + LOCA tests are discussed.

ANALYTICAL MODELING BASIS

These calculations are performed with the ANACAP-U [James, 1997] concrete and steel material behavior model coupled to the ABAQUS [Hibbitt, 1997] general-purpose finite element program. The methodology uses implicit finite element formulations and very detailed continuum analysis that predicts structural response through the modeling of material behavior at each integration point. The ANACAP-U concrete material model is a modern version of the classic smeared cracking model [Rashid, 1968] and can account for the progressive accumulation of damage and associated stiffness degradation. The concrete material model allows cracks to form in three mutually orthogonal directions at each integration point with the crack directions dictated by the principal stress and strain states during loading. Crack initiation is based on an

interaction criterion between principal stress and strain, which allows the development of direct, shear, and split cracking under multiaxial loading conditions. Once a crack forms, it can never heal, but it can close to carry compressive loads and reopen under the cyclic conditions of seismic motion. In compression, the model uses a modified Drucker-Prager yield surface with strain softening behavior in the compression regime after the material exceeds its compressive strength. Hysteretic unloading and reloading behavior in this regime is also included to account for the stiffness and strength degradation under cyclic load. Of considerable importance for these calculations is the modeling for shear performance across a crack. The model accounts for shear transfer due to aggregate interlock with a reduced shear stiffness across a crack as a function of crack opening stain. For a closed crack under compressive load, the model regains its full shear capacity. The model currently does not account for the rebar dowel action. The PCCV model test will provide a challenge for the analytical shear behavior simulation.

The three-dimensional finite element mesh used for these dynamic calculations is shown in Figure 2. The number of elements as well as element types were investigated for mesh sensitivity. The 180° model assumes symmetry across the diametric buttresses and includes the equipment hatch (EH) penetration. Explicit modeling for the lead weights encased in steel shells, as seen in the figure, makes it possible to simulate rocking that may develop due to the distribution of mass. The symmetry conditions, of course, prevent rocking perpendicular to the direction of shaking as well as twisting. Examination of the test data indicated that some rocking about the symmetry plane did occur in the test but that this response was small and did not substantially affect the calculations. The steel liner and other steel plates are modeled with membrane type shell elements as illustrated in Figure 3. This modeling accounts for the inplane shear stiffness of the liner but ignores the liner's out-of-plane small bending stiffness. The "T" stiffener type anchorages are not explicitly modeled for this global model, although the anchorage axial area is included by smearing the area into the liner thickness. The liner is connected to common nodes on the concrete continuum elements, which represents full and continuos anchorage of the liner to the concrete. The prestressing tendons and reinforcing bars are explicitly modeled and imbedded at appropriate locations in the concrete, as illustrated in Figure 4. The hoop tendons are modeled as fully bonded (strain compatible) to the concrete with the justification that friction due to curvature of the PCCV wall will minimize sliding of these tendons under rapidly changing dynamic loads. The straight axial tendons are modeled as unbonded truss elements extending the complete length of the PCCV. All hoop and axial reinforcing bars are modeled as truss-type subelements embedded in the concrete and fully bonded. Stirrup bars tying across the wall thickness and the basemat reinforcement are also included. Material plasticity in the liner, reinforcement bars, and prestressing tendons is considered but certainly not likely in the design level earthquakes.

In the analytical model, the basemat is rigidly attached to the shaking table. A ring of the basemat encompassing the junction of the PCCV wall is thus modeled with the acceleration input applied to the nodes along the bottom and cut surfaces of the basemat. For these post-test calculations, the actual accelerations that were recorded on the basemat in the tests (rather than the target inputs) are used as loading input for the model. Implicit, nonlinear dynamic analyses are performed in series for the sequence of tests to evaluate the time dependence and extent of cracking. The objective is to evaluate the calculated response relative to test data for a given base motion on the structure. The recorded accelerations on the basemat near the buttresses

indicate that some rocking of the basemat does occur. This rocking is included by constructing a node in the center of the basemat and rigidly connecting the surface nodes on the basemat to this central node. An angular acceleration time history is constructed from the difference of the vertical acceleration records and the separation distance. This rocking component is then applied to the central control point. The vertical and horizontal acceleration inputs are constructed from averages of the recorded acceleration data in the respective directions. The drift in displacements, especially for the rotational component, was minimized through low frequency filtering of the input acceleration histories. Examples of the applied acceleration input are shown in Figures 5 and 6.

The post-test calculations use material data input based on test data provided by NUPEC. Nonlinear stress-strain relationships for liner, tendon, and rebar material are used. For the concrete, a uniaxial, static stress-strain curve up to the compressive strength forms the basis for material input. Other input parameters such as tensile cracking strain are based on standard ACI formulas and Raphael's formulas [Rafael 1984] that increase the tensile strength to account for strain rate effects.

ANALYSIS RESULTS

The analytical simulations of the three tests are performed in sequence to allow for the effects of damage accumulation. Each seismic simulation has a duration of about 19 seconds. A full dynamic analysis is conducted for the input acceleration history applied to the basemat using the Hilber-Hughes time marching integration operator. At the end of each seismic input motion, a static step is performed to remove any remaining inertial loads and vibratory motion, and an eigenvalue extraction is performed on the current state to evaluate structural stiffness degradation. The next dynamic analysis is restarted from the previous simulation. Figures 7 through 10 illustrate the results compared to test data for these calculations for various response variables, including the horizontal displacement of the top section relative to the basemat and strains in the liner and reinforcing bars. Figures 11 through 13 show the extent of cracking predicted in the calculations relative to that observed in the tests. The cracking patterns are plotted by drawing a circle in the plane of the crack for the affected integration points. The size of the circle is related to the element size so that the diameter is roughly the tributary area of the integration point. For this smeared cracking methodology, the crack width is predicted by looking at the concrete strains in the area of cracking and multiplying by a characteristic distance, typically the rebar spacing. In the test model, a vertically oriented crack developed in the basemat at the PCCV wall junction after the S1(H+V) test. This bending type crack appeared to be larger around the buttresses but extended around most of the perimeter. The analysis predicts bending dominated cracks developing in the wall-basemat juncture near the buttresses. Most of these cracks close after the motion stops. For the S2(H+V) simulation, the analysis predicts additional cracks to develop in this area plus some cracks to develop near the equipment hatch (EH) penetration. This cracking is confirmed by the test. In the S1(H+V)+LOCA simulation, vertically oriented cracks form in the wall near the buttress. These cracks remain open but are very tight cracks with widths of about 0.01 mm. Similar type cracking is observed in the test specimen. The test specimen also shows cracking in the top portion of the wall near the upper masses, which is not predicted in the analysis. These cracks are attributed to the local "hammering" of the wall by the top mass. Table 1 summarizes the peak horizontal accelerations

and displacements and the fundamental frequencies for the test and the calculations. The calculations generally show the correct characterization but smaller response. This is attributed to differences in damping characterization between the analysis and test. After these calculations were conducted, the test data was evaluated for damping exhibited by the test model. This evaluation indicates that damping was initially about 1% of critical and increased to 1.5 or 2% during the design level test series due to cracking. The calculations reported here used 3% uniform and constant damping. The agreement with the test data is much better for the failure level series of tests in which the damping increases to about 3% due to continued cracking damage. Further calculations are planned to investigate the effects of damping characterization.

Table 1. Summary of Analysis and Test Data

	Peak Horizontal Acceleration (g)		Peak Horizontal Displacement (mm)		Fundamental Frequency (Hz)	
	Test	Analysis	Test	Analysis	Test	Analysis
S1(H+V)	1.19	1.02	2.80	2.16	10.8	11.4
S2(H+V)	1.57	1.31	3.90	2.87	10.3	11.3
S1(H+V) + LOCA	1.03	0.82	2.73	1.80	9.90	11.3

SUMMARY AND CONCLUSIONS

The data collected for the PCCV scale model tests for design level seismic simulations provides an opportunity to benchmark current nonlinear analysis capabilities for this complex problem. The test data confirms that cracking damage and nonlinear material behavior can develop in these types of structures under design level seismic loads. The data also shows that the structural performance is not significantly altered by the cracking, which implies that linear assumptions used in design basis calculations should be adequate. Liner strains are seen to be well within the linear range, and the leak tightness of the liner is easily maintained during multiple design level events. In general, the calculations tended to underpredict the test response both for displacements and strains in tendons, liners, and reinforcement. This is attributed to excessive damping used in the calculations. As expected, the calculations are sensitive to material property data and loading input, but for the input used, the calculations give reasonable overall response predictions, including the general extent of cracking. As such, the calculations verify that the cracking induced during the design level seismic loading does not compromise the performance of the structure for this case. The benefit of such a calculation is to provide a verification for design assumptions that initiation of cracking does not lead to progressive deterioration. The complexity of the nonlinear calculation does not encourage using such calculations to replace design type analyses, but their use as verification analyses can be justified to confirm the integrity of the structure under a design basis earthquake. If the nonlinear continuum calculation does not show significant structural response changes as cracking develops, confidence is gained in the safety of the structure for that loading. However, if the verification calculations indicate a progressive deterioration of the structural performance, serious concerns about the performance and integrity of the structure should be addressed.

ACKNOWLEDGMENTS

The analysis work was funded by the USNRC through Sandia National Laboratories Contract AS-9001. SNL is operated by the United States Department of Energy under Contract DE-AC04-94AL 85000. The results described herein are based on analytical predictions performed at ANATECH and do not necessarily reflect the opinion of the USNRC or NUPEC.

REFERENCES

James, R. J. et al, 1997, ANACAP-U, ANATECH Concrete Analysis Package, User's Manual, Version 2.5, ANATECH Corp., September 1997.

Hibbitt, D. et al., 1997, ABAQUS/Standard User's Manual, Ver. 5.6. Hibbitt, Karlsson, and Sorensen, Inc.

Rashid, Y. R., 1968, "Ultimate Strength Analysis of Prestressed Concrete Pressure Vessels," Nuclear Engineering and Design, 7, pg 334-344.

Raphael, J. M. 1984, "Tensile Strength of Concrete" ACI Journal 81-17, March-April, 1984.

Photograph Courtesy of NUPEC

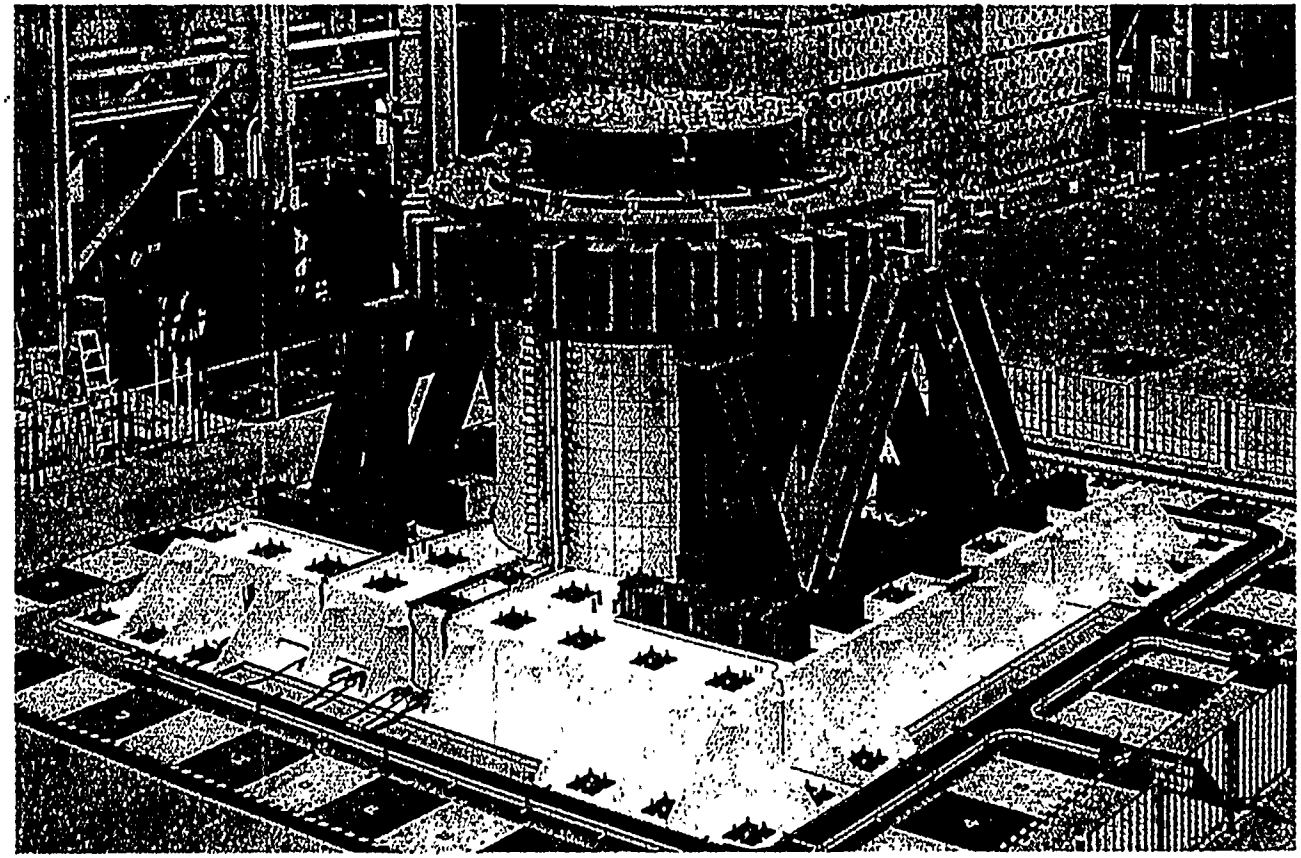

Figure 1. PCCV Test Model on Shaking Table at Tadotsu Engineering Laboratory

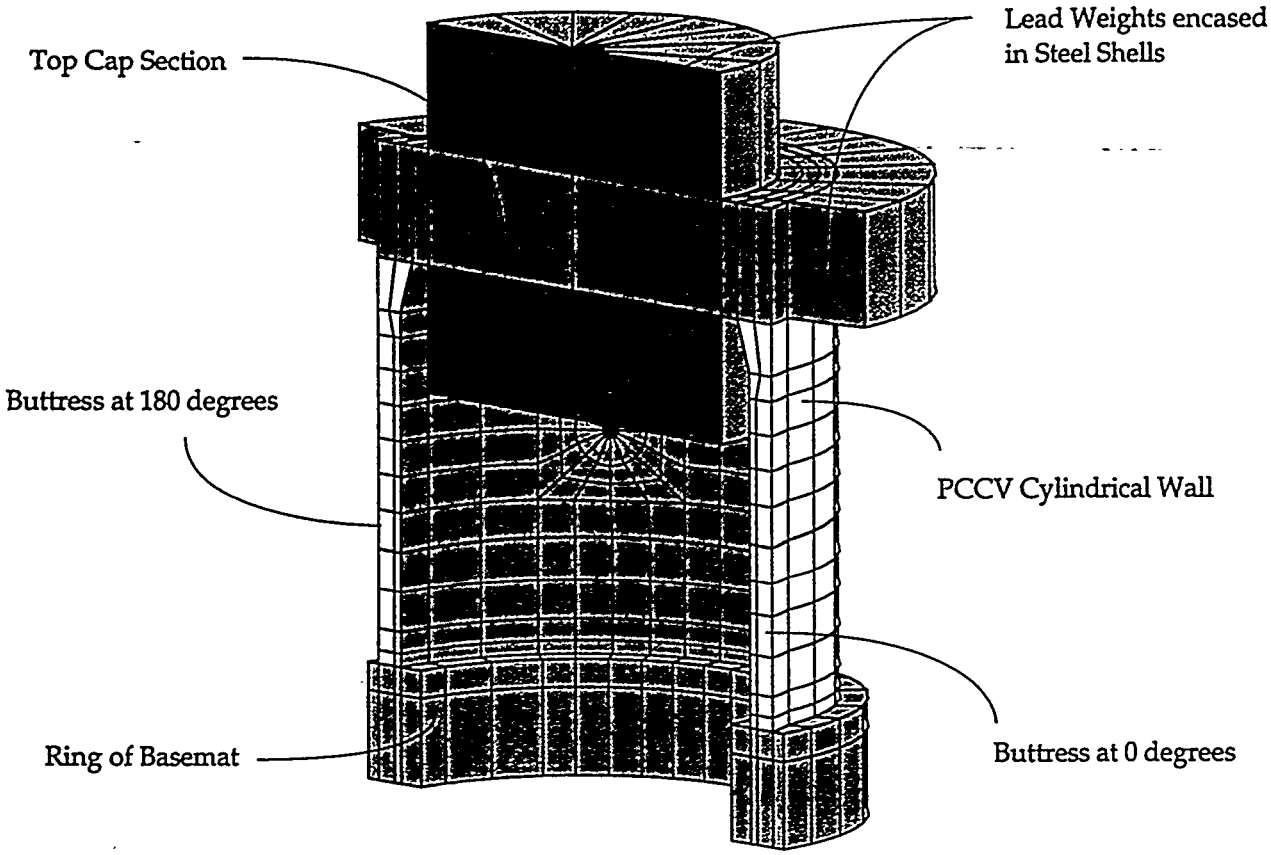

Figure 2. 3D Finite Element Model for Seismic Calculations

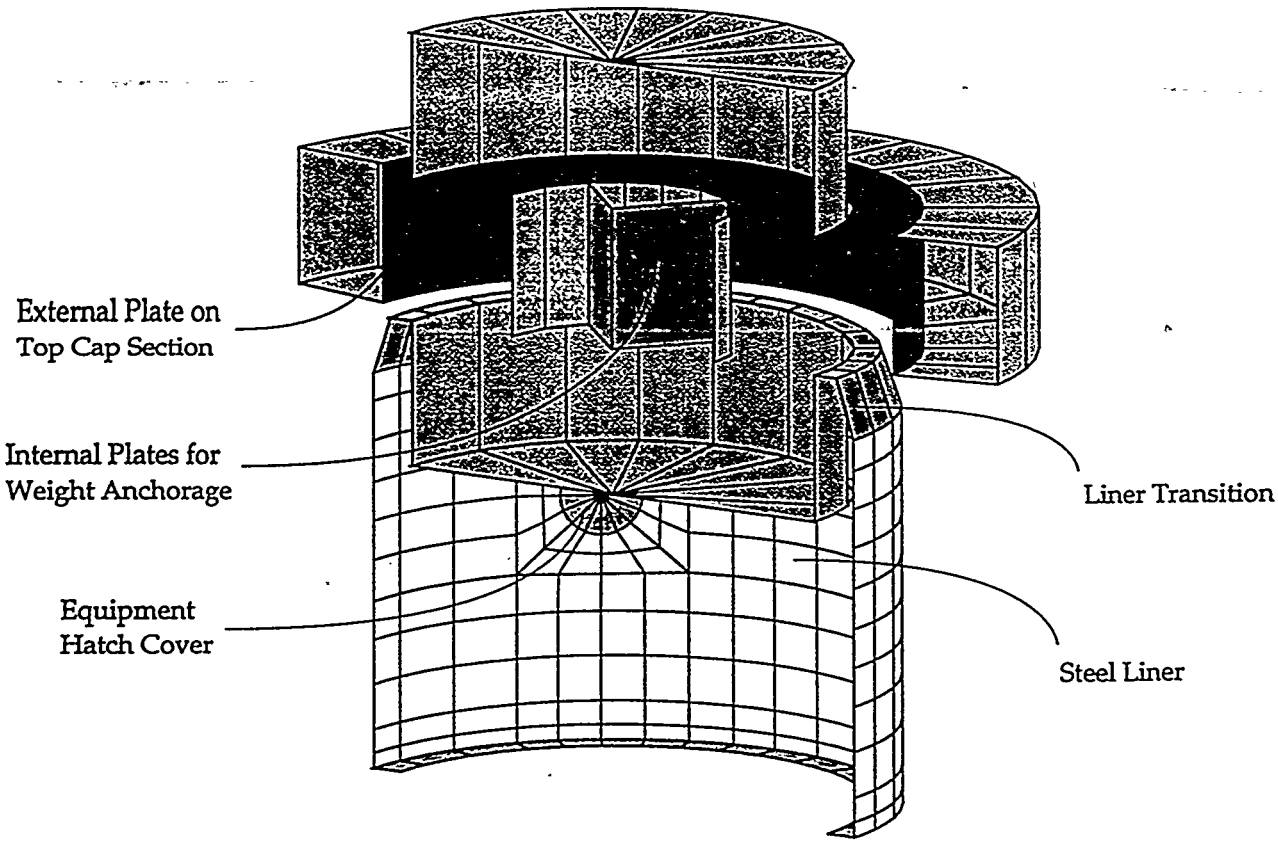

Figure 3. Modeling for the Liner and Steel Plates

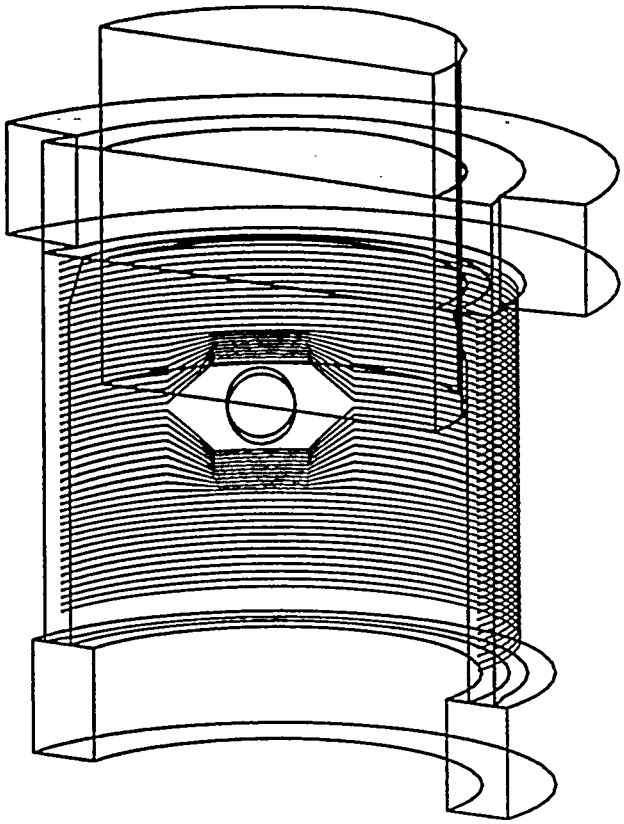

Hoop Tendons

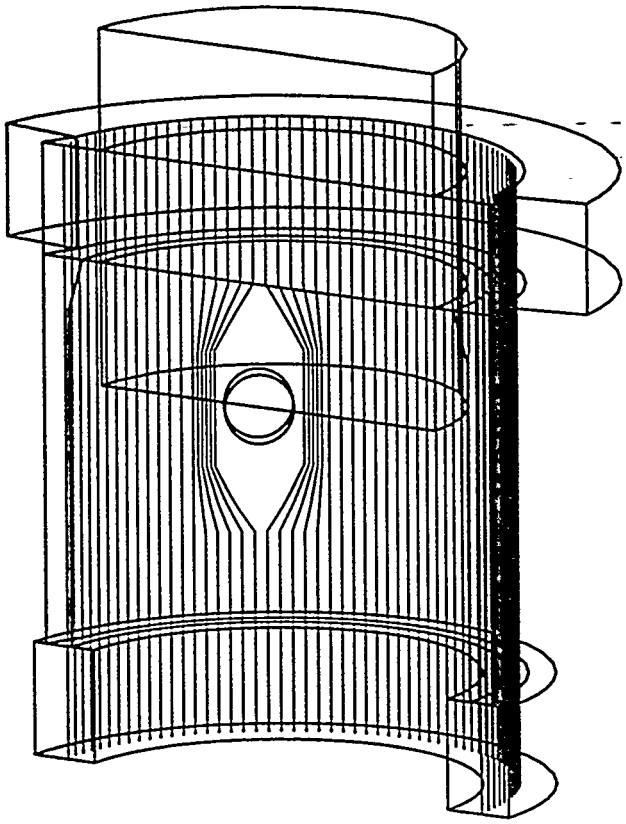

Axial Tendons

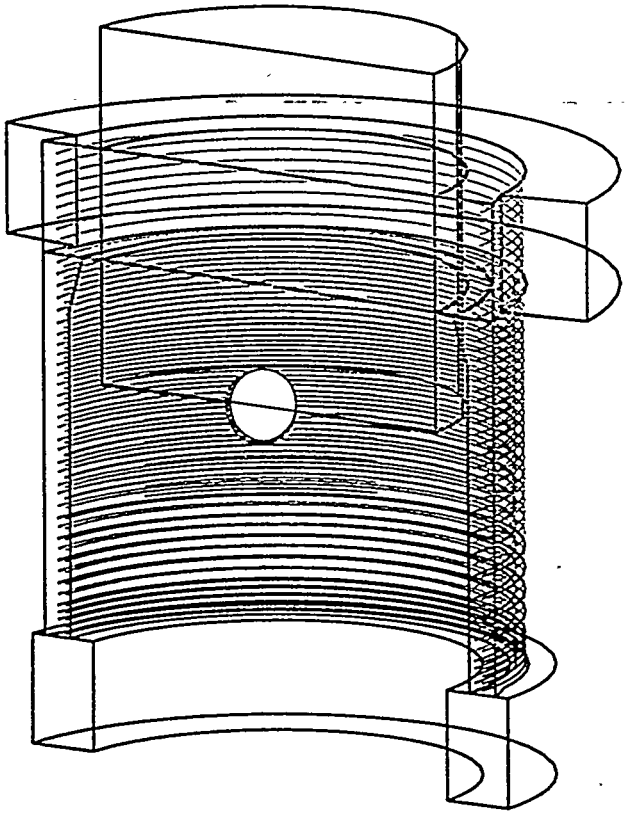

Hoop Rebar

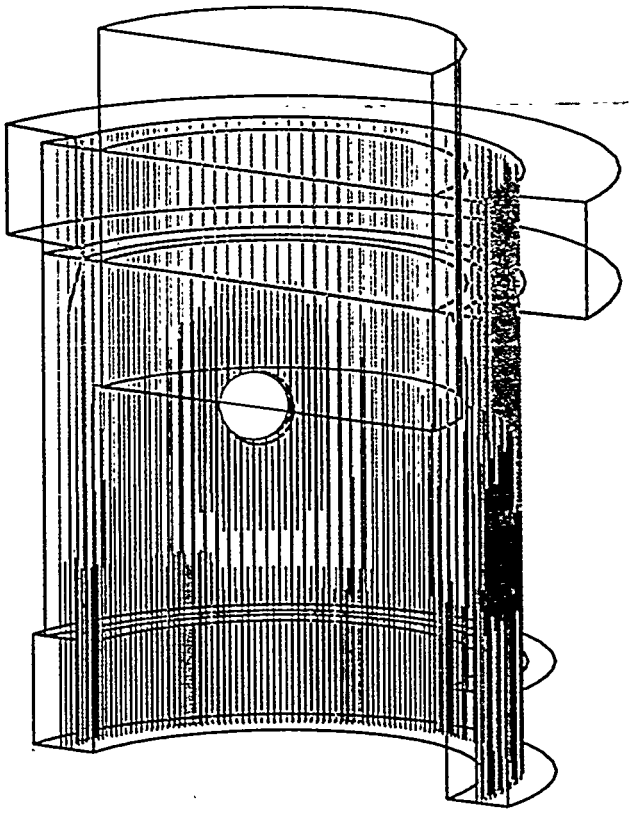

Axial Rebar

Figure 4. Modeling of Prestressing Tendons and Rebars

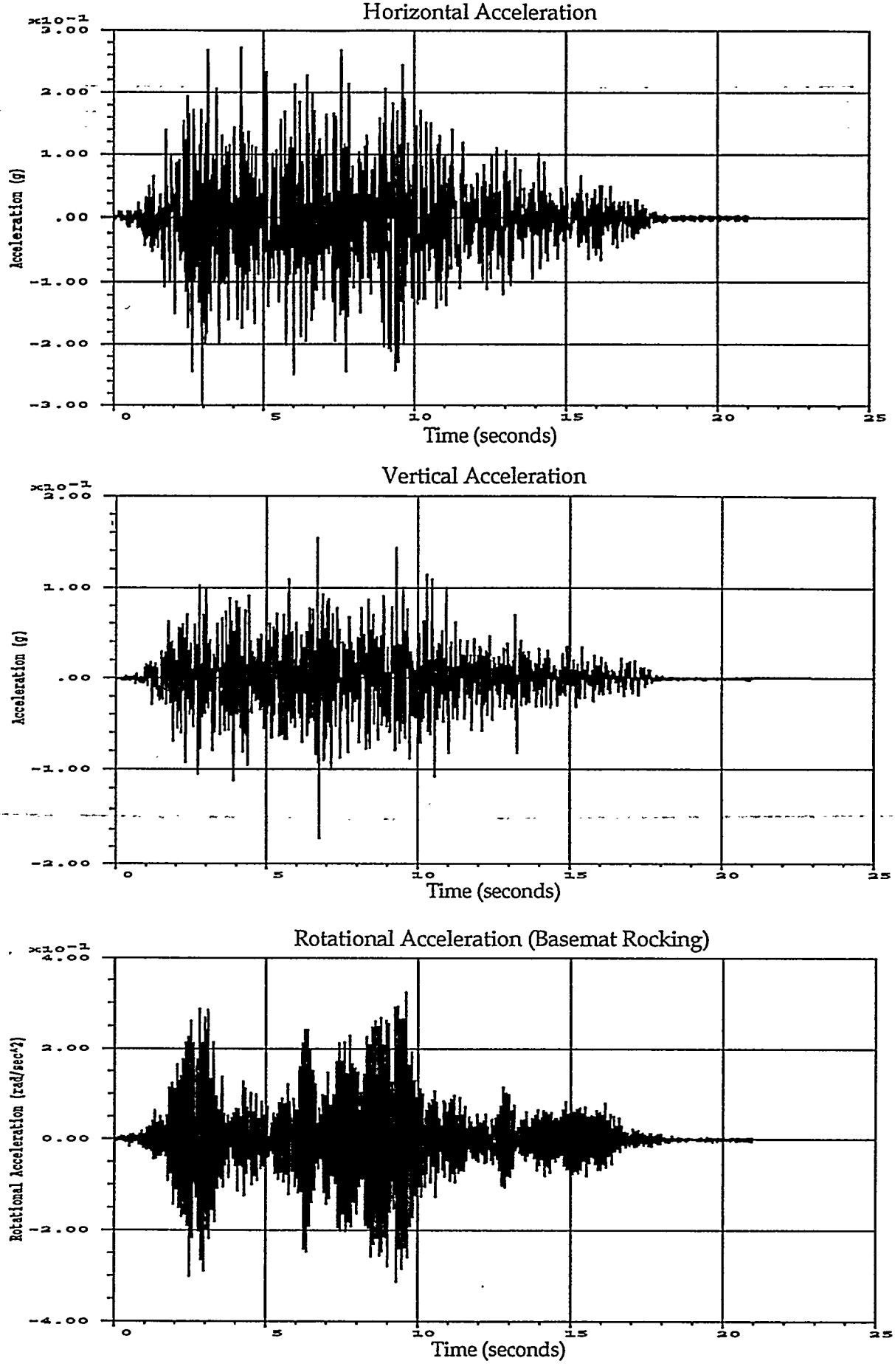

Figure 5. Level S1 Post-test Acceleration Records

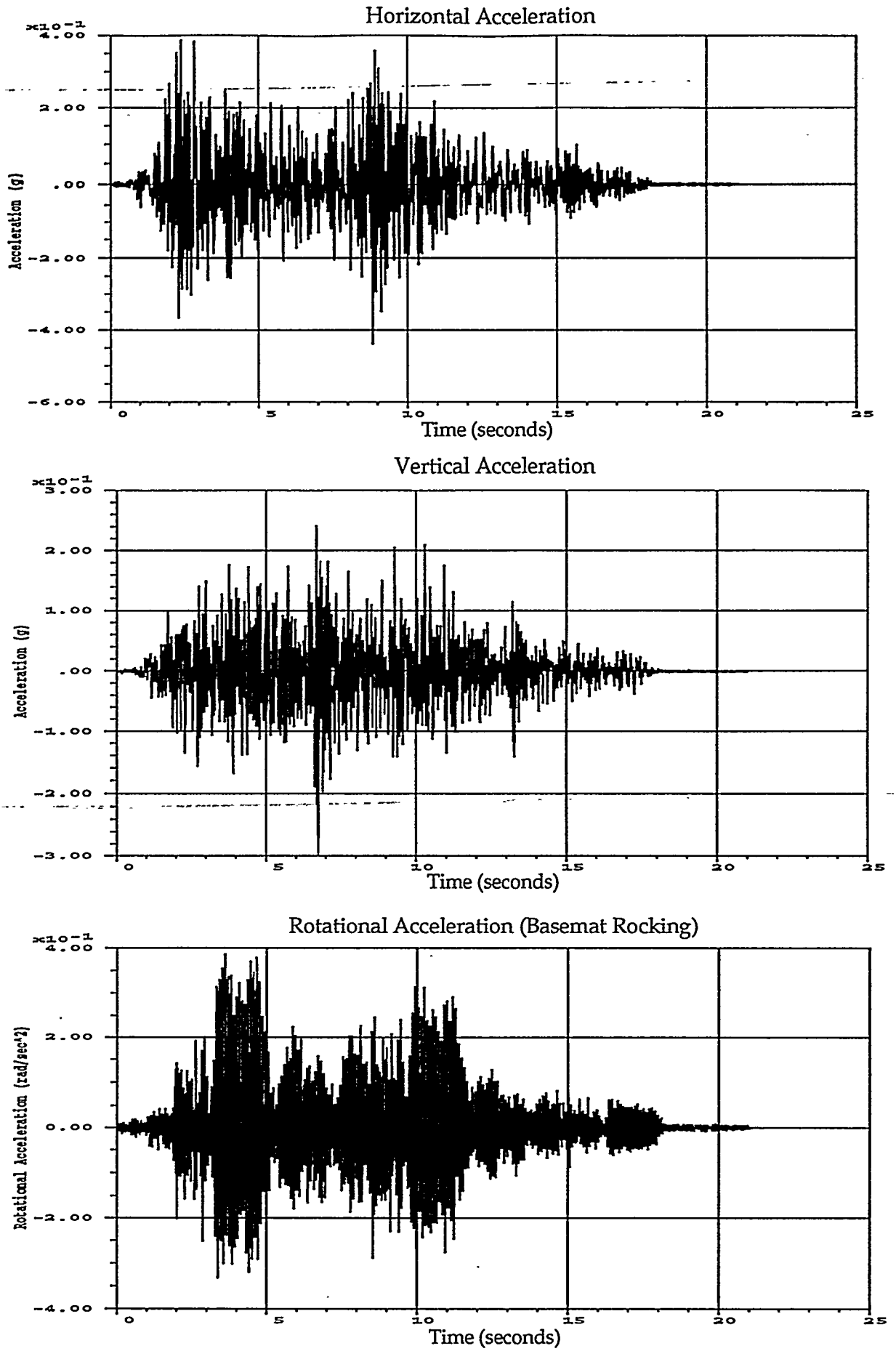

Figure 6. Level S2 Post-test Acceleration Records

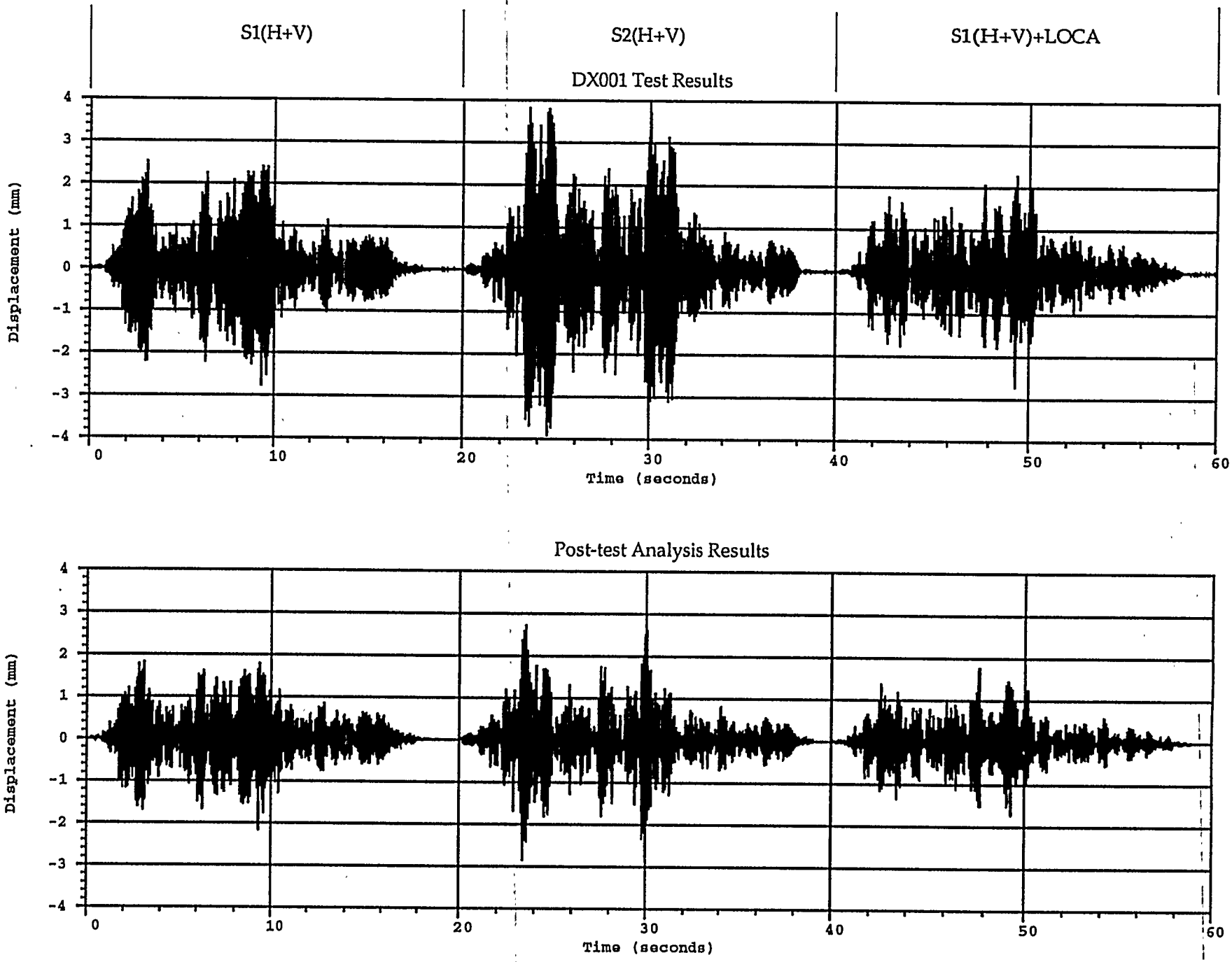

Figure 7. Relative Horizontal Displacement of Top Section under Design Level Seismic Loads

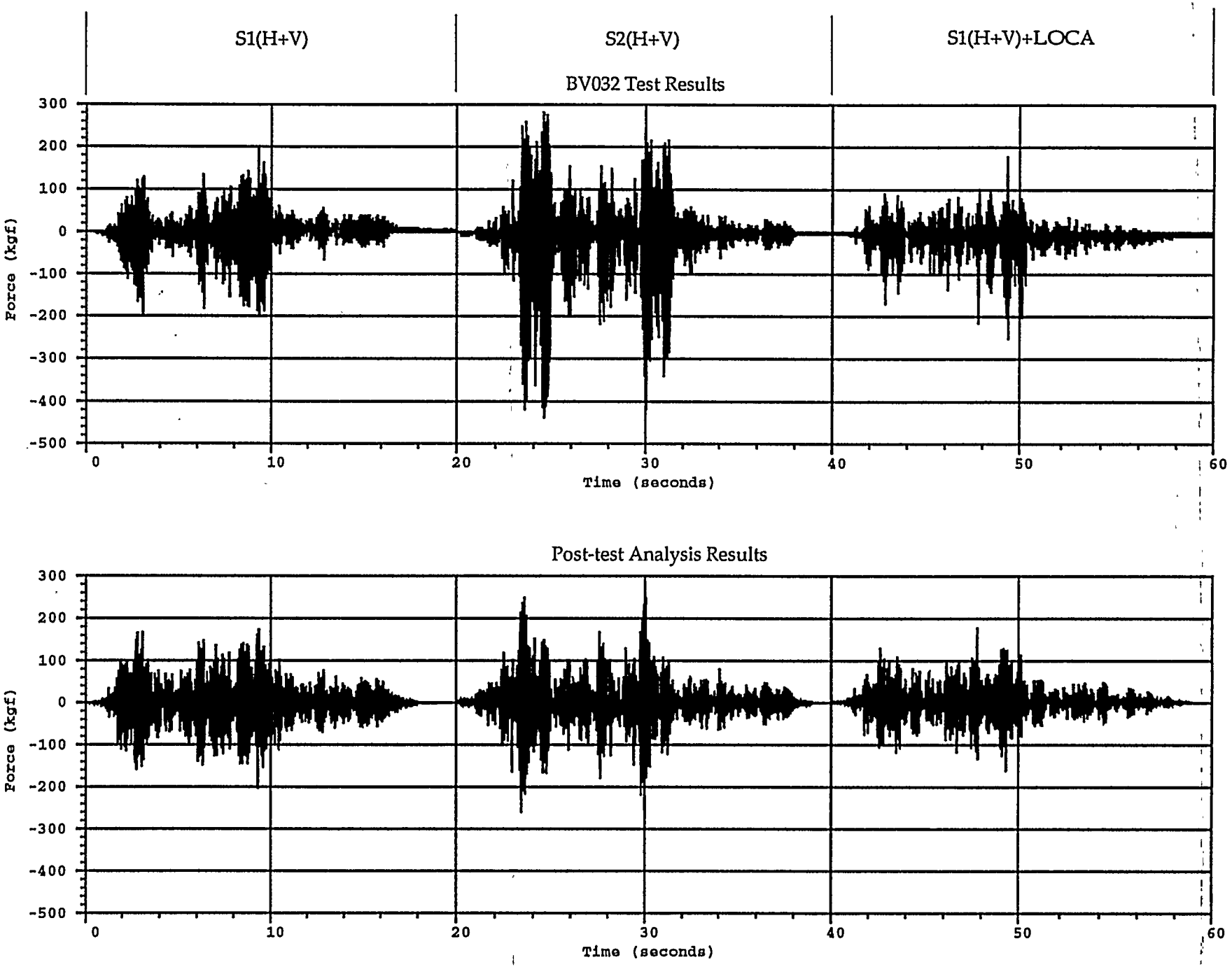

Figure 8. Vertical Tendon Forces at Buttress under Design Level Seismic Loads

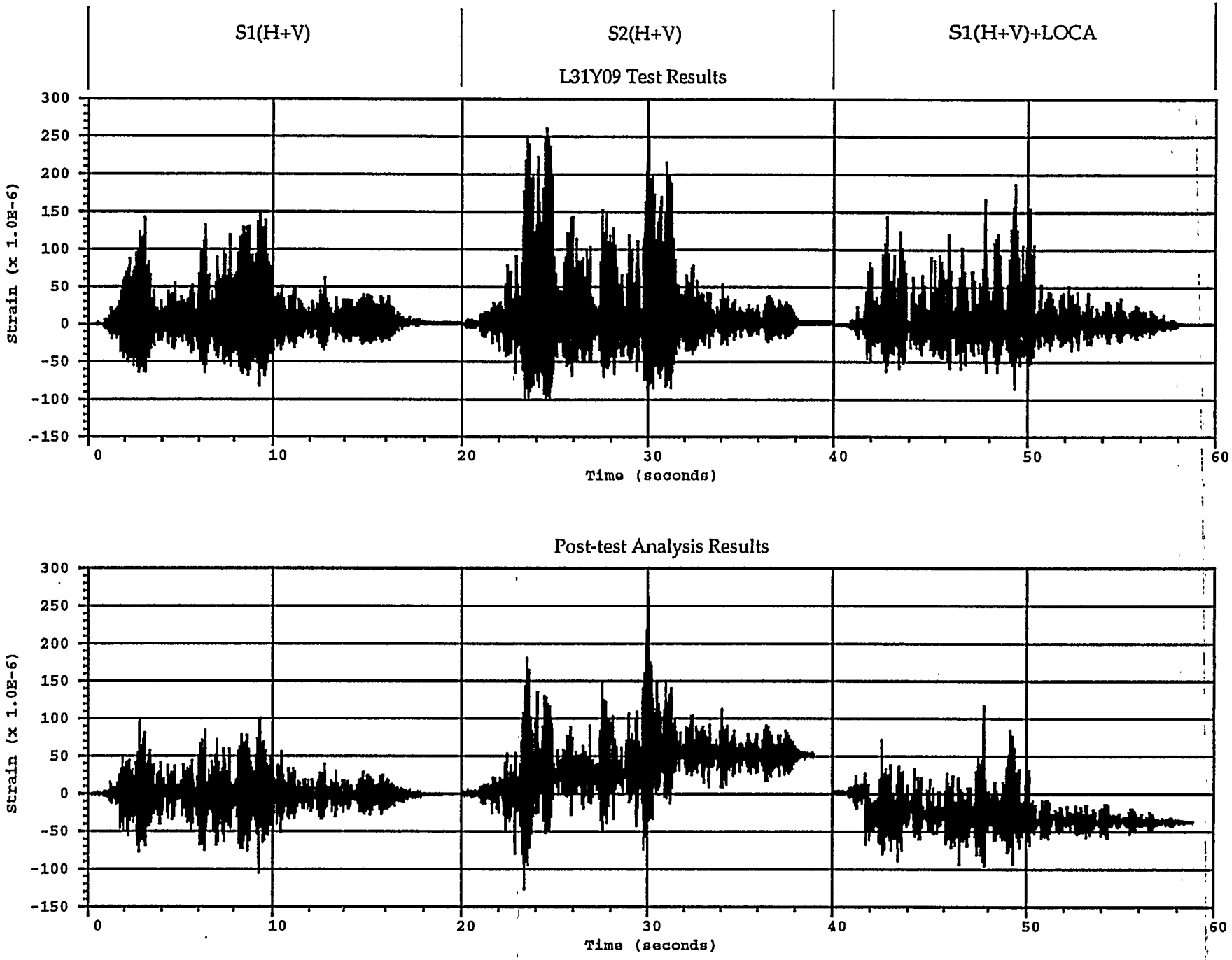

Figure 9. Vertical Liner Strains at Buttress near Wall Junction under Design Level Seismic Loads

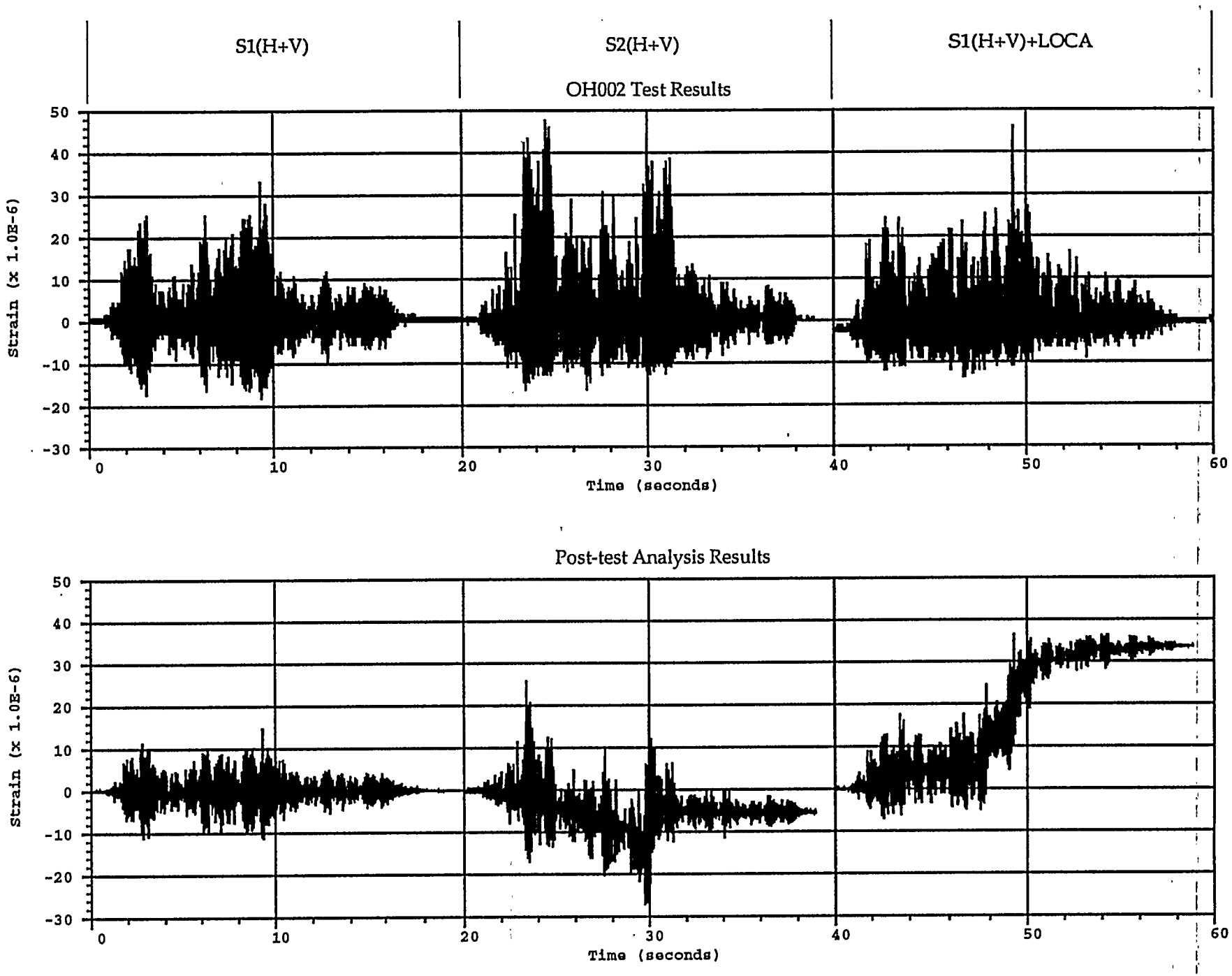

Figure 10. Outside Hoop Rebar Strains at Midheight of Wall under Design Level Seismic Loads

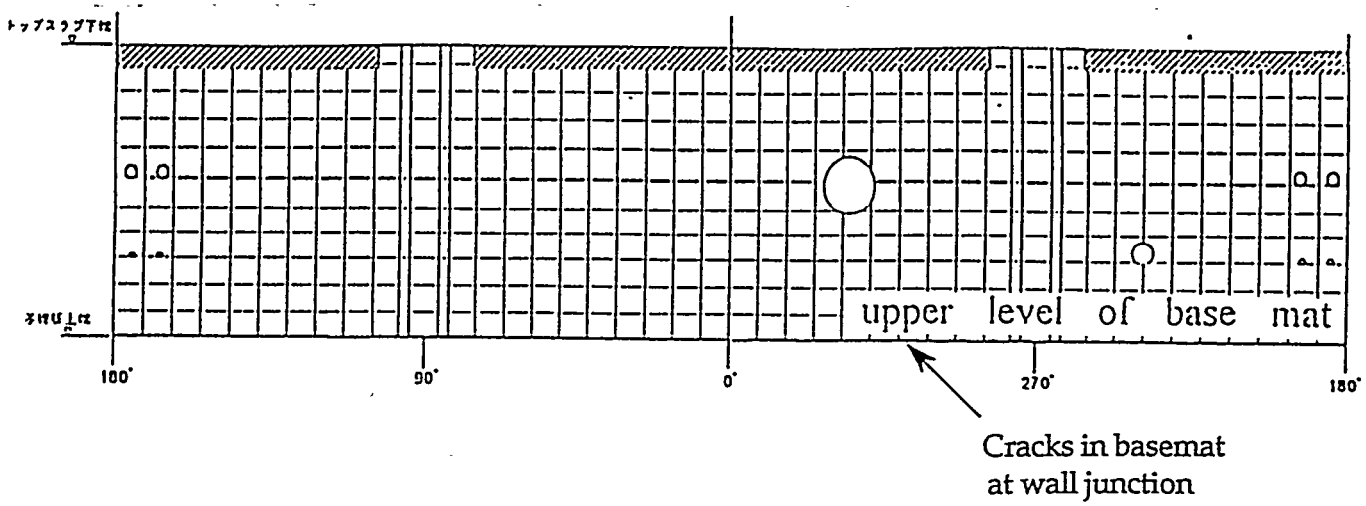

Test

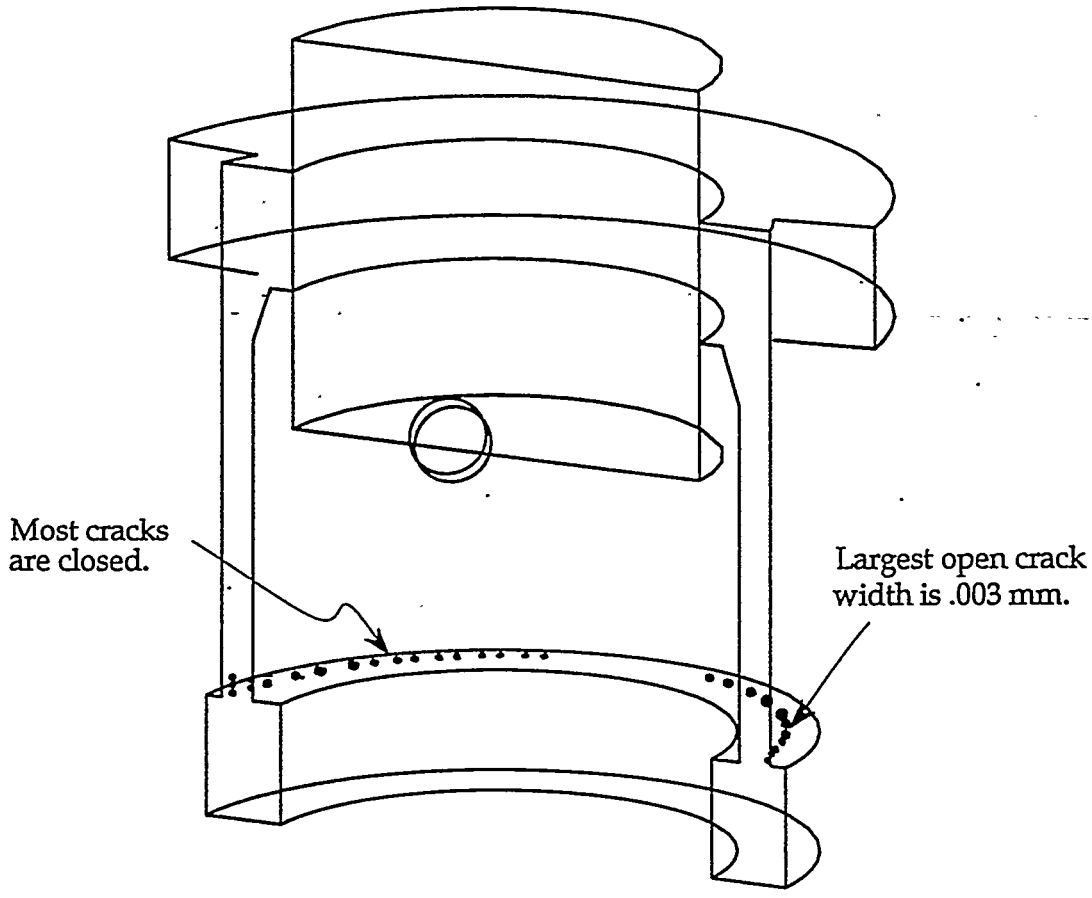

Analysis

Figure 11. Cracking Damage After S1(H+V)

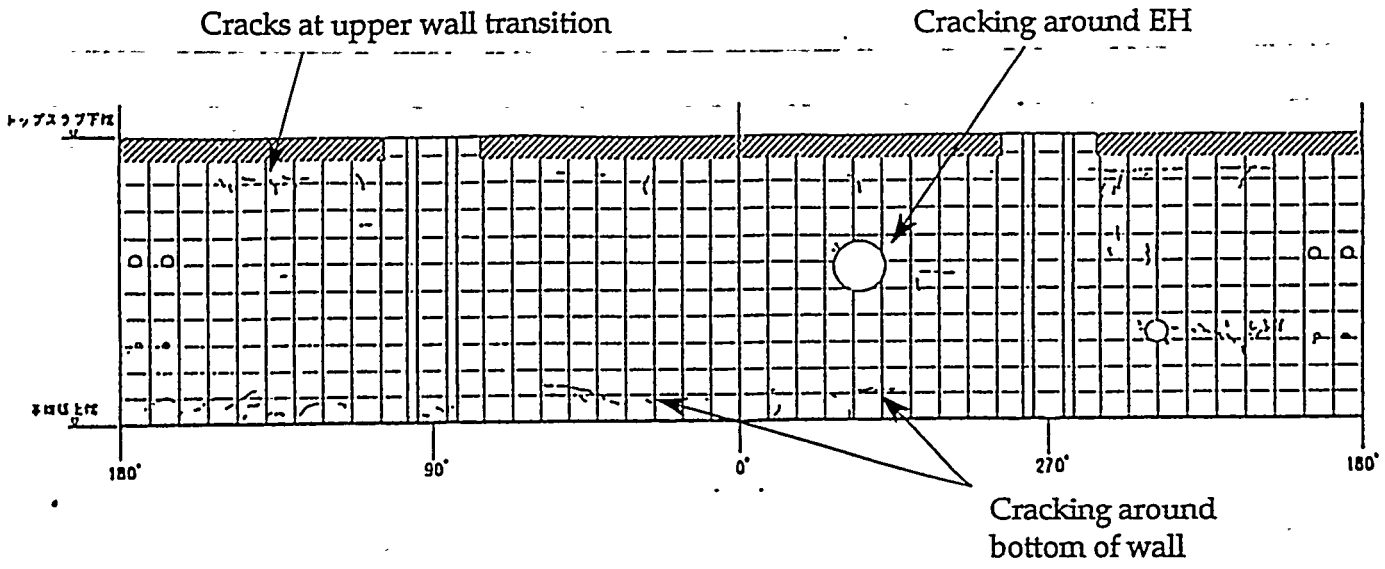

Test

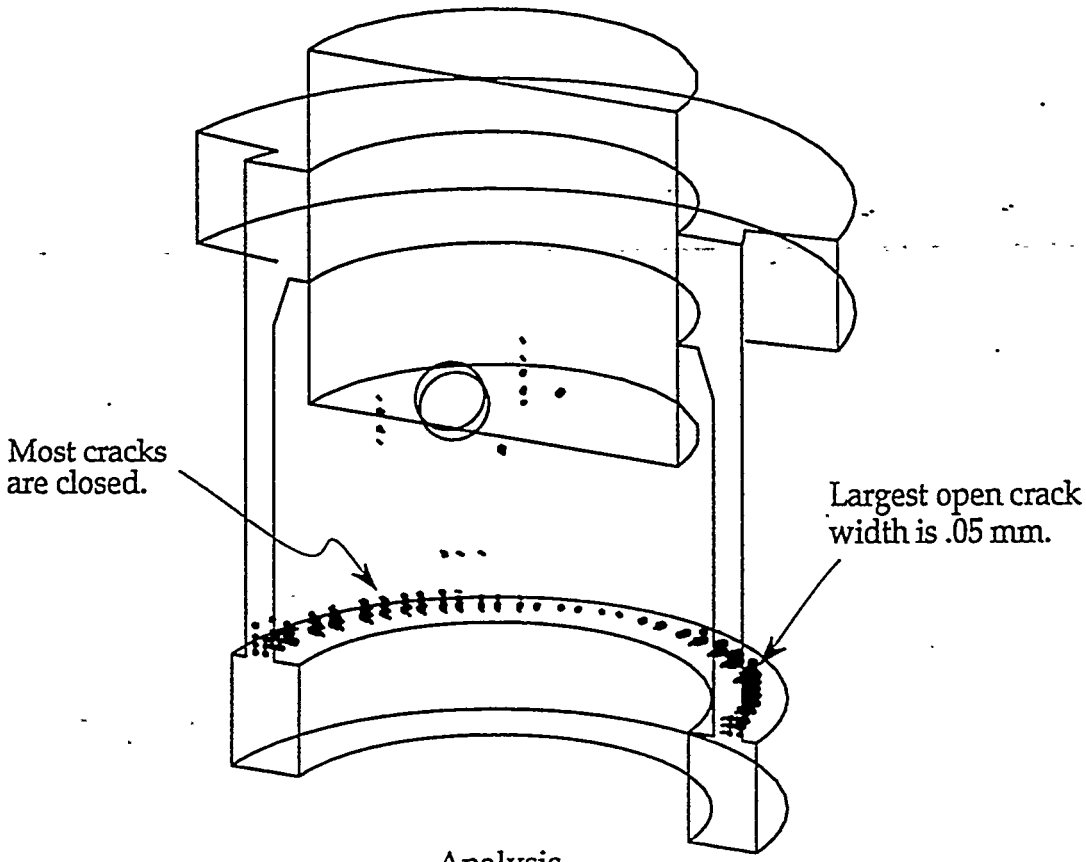

Analysis

Figure 12. Cracking Damage After S2(H+V)

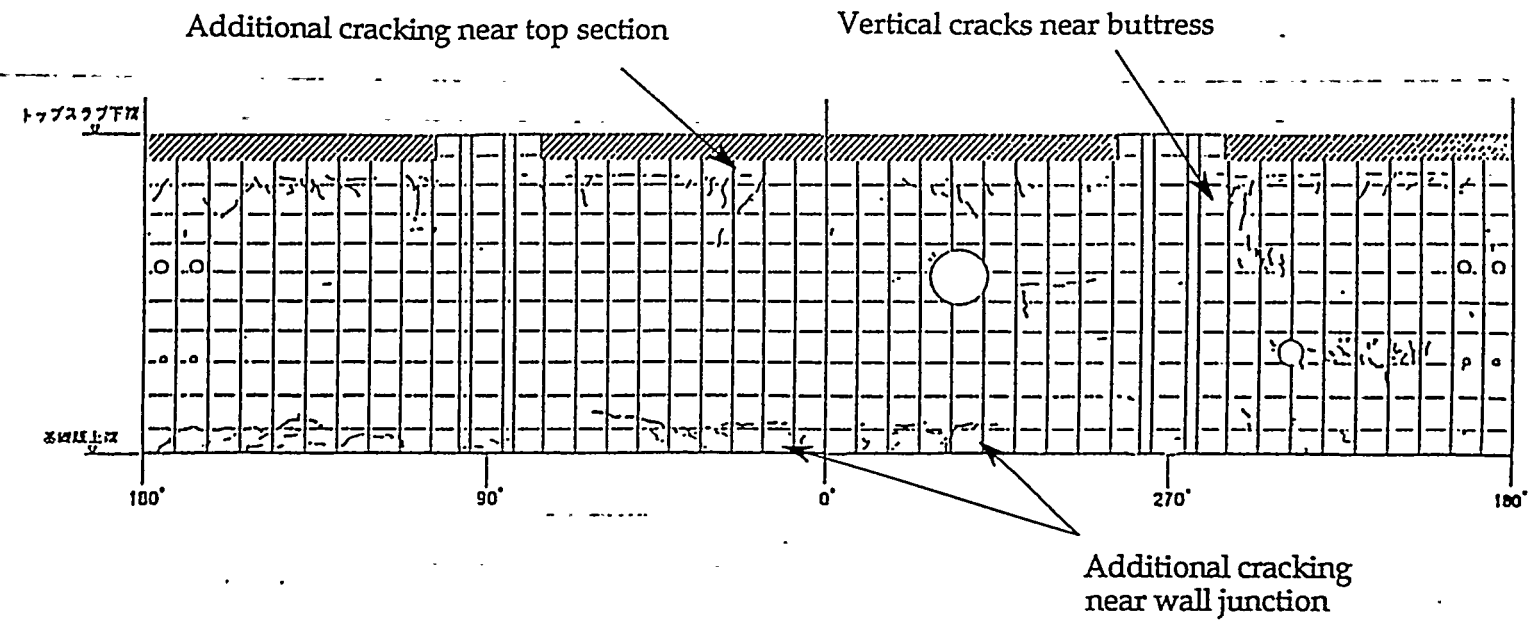

Test

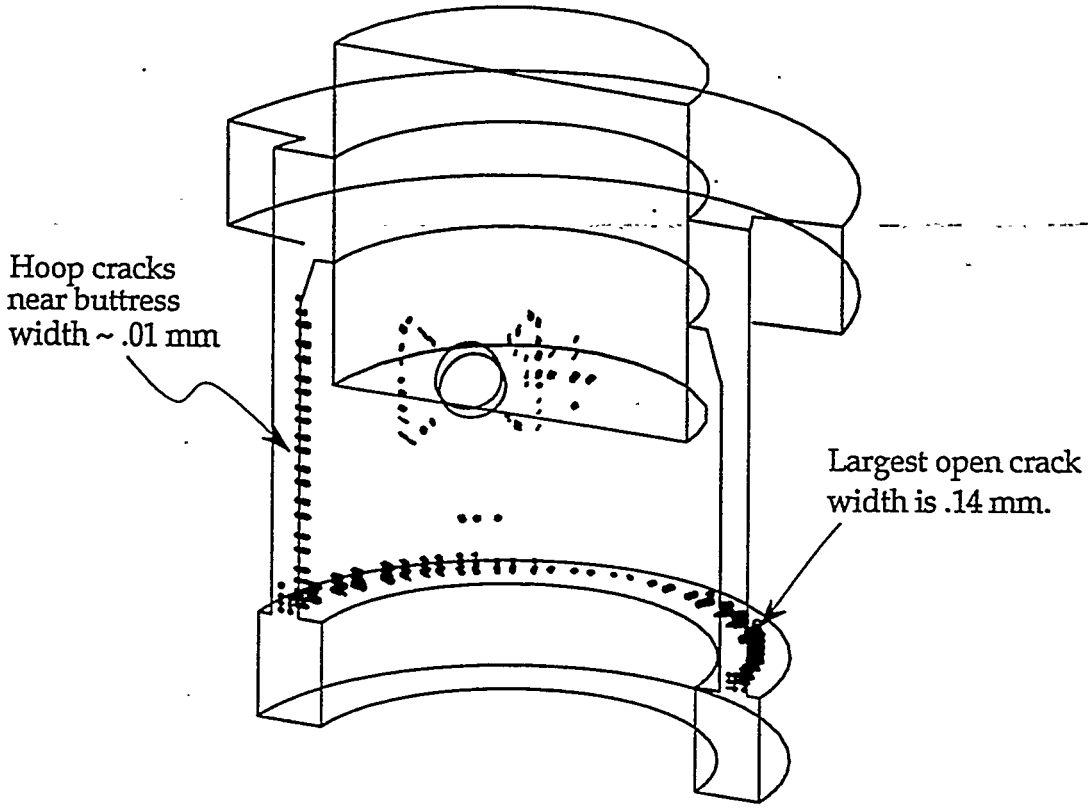

Analysis

Figure 13. Cracking Damage After S1(H+V)+LOCA